Proceedings of Science and Mathematics
Faculty of Science, Universiti Teknologi Malaysia
Vol. 14, 2022, page 8-17

Synthesis of Copper Oxide Nanoparticles from Waste Sim Cards as Photocatalyst in the Photodegradation of Phenol

Elaine Kong Man Yi and Sheela Chandren*
Department of Chemistry, Faculty of Science, Universiti Teknologi Malaysia, Johor, Malaysia
*Corresponding author: sheela@utm.my

Abstract
The high content of heavy metals in most electronic waste (e-waste) had become one of the potential sources that cause environmental pollution and human health issues as electronic devices had been used widely in our daily life. Extraction of heavy metals from e-waste is an effective way to prevent the leaching of heavy metals that harm the environment and human health. In this research, waste SIM cards were used to synthesize copper oxide nanoparticles (CuO NPs) and then utilized as photocatalysts for the photodegradation of phenol under ultraviolet-visible (UV) and visible light irradiations. The elemental composition of waste SIM cards that were analyzed by inductively coupled plasma-optical emission spectrometry (ICP-OES) showed 43.6% of copper (Cu), 2.56% of nickel (Ni), and 0.001% of gold (Au) and iron (Fe). The hydrometallurgy method was used to extract Cu metals from waste SIM cards. Subsequently, a simple wet chemical method was used to synthesize CuO NPs by adding a precipitation agent to the extracted Cu metals, and next the synthesized CuO NPs were washed with an ethanol-water mixture and calcined to remove impurities. Physiochemical properties of the synthesized CuO NPs were analyzed through characterization testing, where Fourier-transform infrared (FTIR) spectroscopy showed an absorption band between 450 to 600 cm^{-1} signifying the formation of CuO NPs. The absorbance spectrum by near-infrared reflectance ultraviolet-visible (NIR-UV Vis) spectroscopy showed the band gap energy was 2.1 eV and X-ray diffraction showed that the CuO NPs are fully crystalline. The photocatalytic testing results showed that the synthesized CuO NPs were capable of degrading phenol under UV and visible light irradiations with the degradation rate of 45.3% and 58.5%, respectively. In conclusion, extracting heavy metals for the synthesis of CuO NPs can help reduce the pollution of e-waste to the environment, and at the same time acts as an effective photocatalyst for the degradation of phenol.

Keywords: E-waste, copper oxide nanoparticles (CuO NPs), photodegradation of phenol

1. Introduction

With exponential advancements made in the field of information technology at the turn of the century, electronic devices proved to play a pivotal role in daily human life. However, this gave rise to an undesirable problem: an increased amount of electronic waste (e-waste). It is estimated that the e-waste generation increased from 44.7 million tons (Mt) in 2016 at a 4 – 5% growth rate per year, reaching 52.2 Mt in 2021. Then, around 20% of e-waste generated in 2016, accounting for 8.9 Mt of electronic waste (e-waste), is documented to be collected and recycled globally, and about 1.7 Mt of residual waste is discarded, with the majority of it being burnt or dumped in landfills in lower-income nations[1]. In general, there is available labour for waste collection in many developing countries, but e-waste is handled in a rudimentary manner due to a lack of infrastructure and cost-effective processes[2]. Significant contamination concerns have been discovered as a result of these hazardous e-waste disposal procedures.

Most electrical and electronic devices might have substances that are hazardous to humans, animals, and the environment, such as heavy metals and halogenated flame retardants [3]. Toxic compounds may be transported into groundwater by landfill leachates, and toxic gases may be released

into the atmosphere by incinerator burning [4]. E-waste pollutants may reach aquatic systems as a result of leaching from dumpsites. The majority of e-waste contains a combination of precious metals, base metals, and toxic metals, including antimony (Sb), silver (Ag), aluminium (Al), gold (Au), arsenic (As), beryllium (Be), bismuth (Bi), cadmium (Cd), copper (Cu), chromium (Cr), iron (Fe), mercury (Hg), nickel (Ni) and platinum (Pt). Besides, e-waste also contains halogens and combustible substances such as plastics and flame retardants[5]. Carcinogens and other harmful metals will be present in the smoke and dust particles produced by e-waste, which cause severe inflammations and lesions, as well as a variety of respiratory and skin illnesses [3]. Hazardous compounds included in e-waste, such as lead, mercury, and chromium, cause a variety of ailments, such as nickel causes skin damage and asthma in particular while antimony causes skin irritation, hair loss, lung, and heart damage, and reproductive issues specifically. In addition, barium weakens muscles, alters heart rate, induces paralysis, and has an impact on the aquatic system [6].

Recycling metal present in e-waste is beneficial for human health and the surrounding, but it also helps alleviate the shortage of resources. One of the recycling methods is to extract the metal present in the e-waste and make use of the metal in other fields such as sensing, bioimaging, and catalytic application. Generally, metal present in the e-waste can be recovered by pyrometallurgical, hydrometallurgical, and biohydrometallurgical methods. The pyrometallurgy method is recovery with thermal treating; this method consumed high energy and high cost but needs a short processing time. The hydrometallurgy method is a recovery method using chemical reagents with low cost and short processing time, but the chances of exposure to toxic chemicals are high. As for the biohydrometallurgy method, it involves the recovery with microbes, which is environmentally friendly but needs a long processing time and specific microbes with selective metal. The extraction method should be selected cautiously according to the laboratory supply, metal to be extracted, and waste management system.

Some researchers have studied the recovery of metals from e-waste, such as Cu from subscriber identity module (SIM) cards, Cu, Ni, Zn, and Co from computer printed circuit boards (CPCBs), as well as Ag and Pd from multilayer ceramic capacitors (MLCCs) [7,8,9,]. Cu is an interesting metal present in e-waste as it is an important nonferrous metal widely used in various fields. Recycling Cu will bring great value to many areas, such as supercapacitor, photocatalyst, and sensing [10]. Cu metal was recovered by hydrometallurgy and biohydrometallurgy methods and then utilized as copper oxide nanoparticles (CuO NPs) for supercapacitor electrode material [8]. CuO NPs have a wide range of applications in nanotechnology, including medicine, biological activity, energy devices, industrial domains, catalysis, and environmental remediation [11].

In this study, Cu metals were recovered from waste SIM cards by the hydrometallurgy method. Then, the physicochemical properties of the CuO NPs were characterized with Fourier-transform infrared (FTIR) spectroscopy, near-infrared reflectance ultraviolet-visible (NIR UV-Vis) spectrophotometer, and X-ray powder diffraction (XRD). Lastly, the photocatalytic performance of the synthesized CuO NPs was evaluated through the degradation rate of phenol solution through detection using a UV-Vis spectrophotometer.

2. Methodology

2.1. Procurement and metal content analysis

First, the metal part of the SIM cards was removed from the plastic and weighed with an analytical balance. Then, the metal part of the SIM cards was crushed into smaller pieces. After that, 0.25 g of the crushed sample was added to about 10 mL of concentrated HCl in a pressurized container. Then, the container was placed into a Millestones microwave oven digestor for digestion. After the microwave digestion, the sample was analyzed with Agilent ICP-OES for the concentration of Cu, Ni, Au and Fe.

2.2. Synthesis of CuO NPs from waste SIM cards

First, the metal part of the SIM cards was removed from the plastic and weighed with an analytical balance. Then, the metal part of the SIM cards was crushed into smaller pieces. After that, the sample was washed with distilled water. Then, the cleaned sample was placed into a 150 mL three-neck round bottom flask and added 50 mL of concentrated HCl and concentrated HNO_3 mixture with a ratio of 1:1. Then, the mixture was stirred with a magnetic stirrer at room temperature for 6 h until the sample was

completed leached. Then, a few drops of 8 M of sodium hydroxide (NaOH) were added dropwise into the mixture until black precipitate and refluxed at 100 ℃ for 24 h. After 24 h, the solution was cooled to room temperature. Then, the mixture was distributed into four centrifuge tubes for washing with the ethanol-water mixture. The solution was centrifuged for 7 mins thrice to separate the precipitate formed. The centrifuge tube was then covered with aluminium foil and dried in an oven at 80 ℃ for 24 h. Lastly, the precipitate obtained was calcined in an open container at 450 ℃ for 6 h using a furnace.

2.3. Characterizations of CuO NPs

2.3.1 Fourier-transform infrared spectroscopy (FTIR)

Perkin Elmer Spectrum 1600 FTIR spectrometer was used to record the FTIR spectra. The potassium bromide (KBr) method was used where the samples with KBr were grounded using mortar and pestle to obtain a homogeneous powder with the samples to KBr ratio of 100:1. Then, the powder mixture was pressed with 8 tons of pressure for 5 mins, forming a disc-shaped sample. Lastly, the sample was placed into the sample holder, and the spectra were recorded within the range of 400 – 4000 cm^{-1}.

2.3.2 X-ray diffraction (XRD)

The samples were characterized using XRD to determine their crystallinity, structural phase-type with content, and crystallite size. Rigaku X-ray diffractometer (SmartLab model) with Cu Kα radiation (λ = 1.5418 Å) was used, operating at 40 kV and 30 mA. The diffraction pattern was set in the 2θ range of 20˚ to 80˚. The average crystalline size was calculated with the Debye Scherrer equation, as shown in equation 1.

$$D = \frac{K\lambda}{\beta \cos \theta} \quad (1)$$

2.3.3 Near infrared reflectance ultraviolet-visible (NIR-UV-Vis) spectroscopy

Spectroscopy Shimadzu NIR UV-Vis spectrophotometer with model UV-3600 was used to identify the bandgap energy of the CuO NPs. The CuO NPs were spread into the sample holder and then placed in the spectrometer holder. The spectrum was collected within the wavelength range of 200 to 800 nm. The bandgap energy was then determined by the Tauc plot method.

2.4. Photodegradation of phenol with CuO NPs as the photocatalyst

First, phenol solutions with the concentration of 20 ppm, 40 ppm, 60 ppm, 80 ppm, and 100 ppm were prepared. 0.025 g of phenol detached crystal was weighed and diluted with acetonitrile in a 25 mL volumetric flask for the preparation of the 1000 ppm stock solution. After that, different concentrations of phenol standard solution were prepared by diluting the stock solution in a 10 mL volumetric flask. Then, the solutions were analyzed with a UV-Vis spectrophotometer. The reading obtained was used for the plotting of the calibration curve. For the photocatalytic reaction, 50 mL of 100 ppm phenol solution was added to a test tube. Then 0.05 g of CuO NPs was added to the solution and placed in dark conditions for an hour to allow for absorption. The irradiation of light was carried with a 6 W UV lamp as the UV light source and Philip 18 W light-emitting diode (LED) lamp bulb as the visible light source. The solution was placed for degradation for 5 h. The apparatus set-up was ass shown in Figure 1. After that, the solution was analyzed with a UV-Vis spectrophotometer. The degradation rate was calculated using equation 2.

$$Degradation\ rate\ (\%) = \frac{C_0 - C_t}{C_0} \quad (2)$$

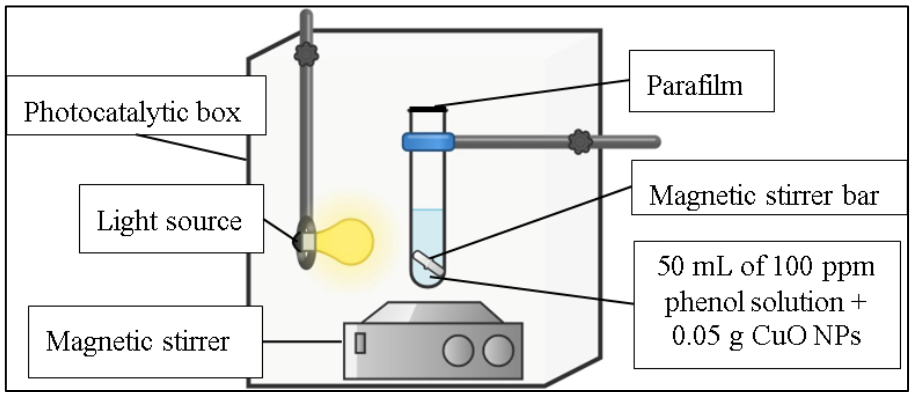

Figure 1. Apparatus set up for photodegradation of phenol

3. Results and Discussion

3.1. Procurement and metal analysis of waste SIM cards

The metal parts of collected waste SIM cards were separated from the plastic body, then it was crushed and digested with a microwave in a closed vessel. After the microwave digestion, the sample was analyzed with ICP-OES for the concentrations of Cu, Ni, Au and Fe. Table 1 shows the result of the metal analysis obtained from ICP-OES. The results obtained from ICP-OES were then used to calculate the percentage of metal contents for the metal part of the SIM cards.

Table 1. Metal content analysis of waste SIM cards

Result from ICP-OES			
Element	Concentration ($x10^3$ ppm)	Concentration per 100g (g)	Percentage (% W/W)
Cu	440.400	44.040	43.600
Ni	24.080	2.408	2.560
Au	0.283	0.028	0.001
Fe	0.243	0.024	0.001

The result showed that the waste SIM cards contain 43.60 % of Cu, 2.56% of Ni, and 0.001% of Au and Fe. The amount of metals obtained was much less compared to the reported results which were 75.84% for Cu, 3.17% for Ni, 0.42% for Au and 1.28% for Fe [12]. One of the possible explanations for this is that the metal part obtained and weighed for the metal analysis also included the glue part that adhered to the metal part. This will lower the percentage of the element since the total weight of the sample had increased, yet the metal content was comparably low. Other than that, the sample might not have dissolved completely during microwave digestion. Hence, the amount of the dissolved metals was less than that in the reported result.

3.2. Synthesis of CuO NPs from waste SIM cards

Synthesis of CuO NPs from waste SIM cards involved the extraction of Cu metals from waste SIM cards by acid leaching, chemical precipitation by adding concentrated NaOH solution, washing and calcination. For the extraction of Cu metals, a mixture of concentrated HCl and HNO_3 with a ratio of 1:1 was used for acid leaching. Figure 3 shows the observation for acid leaching of waste SIM cards. It was observed that the metal part of the waste SIM cards dissolved completely in the acid mixture forming a green solution and evolving a brown gas. The reaction involved in acid leaching is shown in equation 3. From equation 3, the evolved brown gas was nitrogen dioxide (NO_2) gas formed when Cu metals oxidised to Cu(II) ions.

$$Cu + 2HCl + 2HNO_3 \rightarrow Cu^{2+} + 2Cl^- + 2NO_2 + 2H_2O \quad (3)$$

Figure 3. Acid leaching of waste SIM cards

After that, 6 M of NaOH solution was added dropwise to the solution and then heated under reflux at 80 ℃, lastly dried in an oven for 6 h at 100 ℃. Equations 4 and 5 show the reaction that occurred after the addition of NaOH.

$$CuCl_2 + 2NaOH \rightarrow Cu(OH)_2 + 2NaCl \quad (4)$$

$$Cu(OH)_2 \rightarrow CuO + H_2O \quad (5)$$

The green solution was changed to bluish-green and then changed to black when the reaction was completed. Figure 4 shows the observation of colour changes during the addition of NaOH solution. The temperature for decomposition of $Cu(OH)_2$ to CuO NPs was 80 ℃, thus the temperature was maintained at 80 ℃ during the addition of NaOH solution [10]. From past studies, the formation of CuO NPs was pH-dependent where a black solution with CuO NPs will be formed at high pH (12 – 14), while an orange solution with Cu_2O particles will be formed at a lower pH value (lower than 7) [13]. The black solution with CuO NPs was then washed with an ethanol-water mixture to remove the salts present. Then, the obtained black precipitate was placed in an oven to dry the ethanol-water mixture at 80 ℃ for 24 h. Lastly, the dry black precipitate was calcined at 450 ℃ for 6 h in an open container to remove water and by-products that might still be present in the precipitate.

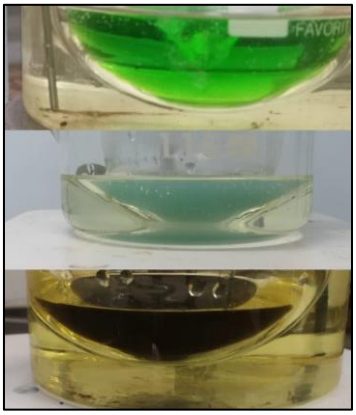

Figure 4. Observation during the addition of NaOH solution

3.3. *Functional group analysis*

TIR had been used to analyze the functional groups present in the synthesized CuO NPs. Figure 5 shows the FTIR spectra for CuO NPs before and after calcination. Both spectra showed two broad peaks at around 3400 cm^{-1} and 1634 cm^{-1} which correspond to the O-H groups. O-H stretching bond of absorbed water and surface hydroxyl located at a broad peak between 3200 and 3600 cm^{-1} as well as asymmetric stretching of O-H bond of water corresponds to the peak around 1637 cm^{-1} [14]. Both spectra also showed the absorption peaks at 1384 cm^{-1}, which corresponds to the stretching of the N-

O bond due to the presence of nitrate, NO_3^{2-} ions [15]. The NO_3^{2-} ions were formed when Cu dissolve in HNO_3, as shown in equation 6.

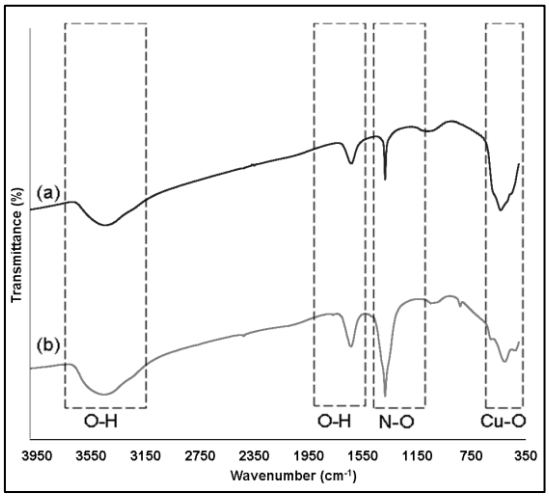

Figure 5. FTIR spectra (a) uncalcined CuO NPs and (b) calcined CuO NPs.

$$3Cu + 8HNO_3 \rightarrow 3Cu^{2+} + 6NO_3^{2-} + 2NO + 4H_2O \quad (6)$$

In the preparation process, calcination is important to enhance the crystallinity of CuO NPs and remove impurities that are present [16]. NO_3^{2-} ions from $NaNO_3$ salts still be present due to insufficient washing, which might take around 4 to 5 times to be completely removed [17]. However, the stretching peak for N-O centred at 1384 cm^{-1} was still present after calcination, which might be caused by the high decomposition temperature of $NaNO_3$ From a previous study, the decomposition of $NaNO_3$ with the evolution of NO and O_2 started at around 450 °C and was significantly over at 680 °C [18]. Thus, calcination at 450 ℃ was insufficient to remove all the $NaNO_3$ that was present. In addition, the higher intensity of N-O peak for the calcined sample was due to the different volumes of sodium hydroxide added since both the calcined and uncalcined samples were prepared in different batches. From the spectra, the uncalcined CuO NPs showed an absorption peak at 533 cm^{-1}, while the calcined CuO NPs showed absorption peaks at 604 cm^{-1}, 504 cm^{-1} and 424 cm^{-1}, which associated with the stretching of Cu-O bond. According to past studies, more significant peaks of Cu-O bond between 400 to 600 cm^{-1} were observed after calcination, which is in good agreement with past studies [16,19].

3.4. Band gap energy determination for CuO NPs

NIR UV-Vis spectrophotometry was used to measure the absorbance of the synthesized CuO NPs. Figure 6 showed the absorbance spectrum for the CuO NPs. The absorbance peak for the synthesized CuO NPs was at 305 nm, which is in good agreement with the previous study showing the absorbance of the CuO NPs at around 300 nm [20]. Following that, from the information from the absorbance spectrum, the Tauc plot was prepared to estimate the band gap energy. Figure 7 shows the Tauc plot for the CuO NPs. The band gap obtained from the tangent line shows that the CuO NPs have a narrow band gap, which is 2.1 eV. According to a past study, the band gap energy for an efficient photocatalyst should be smaller than 3 eV [21]. The observed low band gap energy shows good agreement with previous studies as an efficient photocatalyst with good absorption of visible light. From a previous study, the band gap energy of CuO NPs was estimated to be around 1.2 eV to 2.1 eV at which CuO NPs can generate maximum reactive oxygen species and absorption of visible light with this low band gap energy [21].

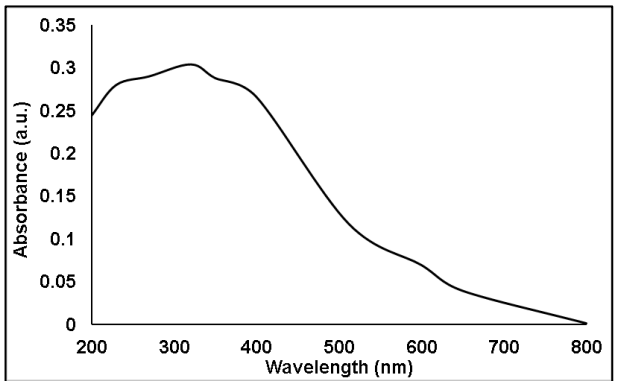

Figure 6. NIR-UV Vis absorbance spectrum for CuO NPs

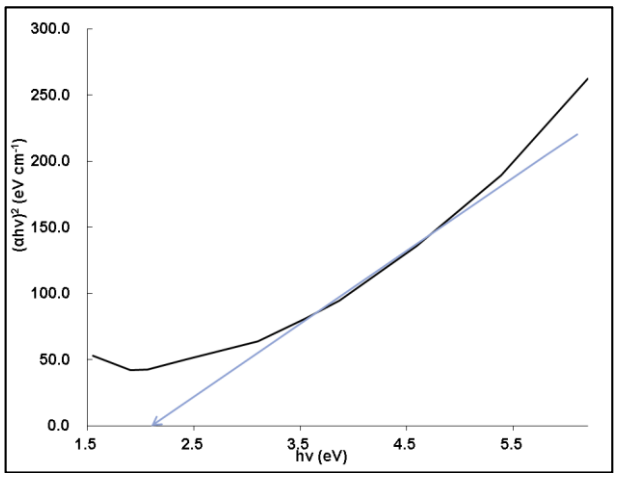

Figure 7. Tauc plot for CuO NPs

3.5. *Crystallinity study by XRD*

In this study, XRD was used for the crystallinity study. As shown in Figure 8, the synthesized CuO NPs showed prominent peaks at 2θ values of 32.6, 35.5, 38.8, 48.7, 58.2, 68.1, 75.3 °, corresponding to the *d*-spacing of 2.74 Å, 2.52 Å, 2.32 Å, 1.86 Å, 1.87 Å, 1.58 Å, 1.38 Å and 1.2 Å, respectively. These diffraction peaks can be indexed to the lattice plane (110), (11-1), (111), (20-2), (202), (113) and (004) respectively. The XRD pattern also proved that the CuO NPs are fully crystalline. The obtained results match well the data obtained from the Joint Committee on Powder Diffraction Standard (JCPDS) file number 45-0937.

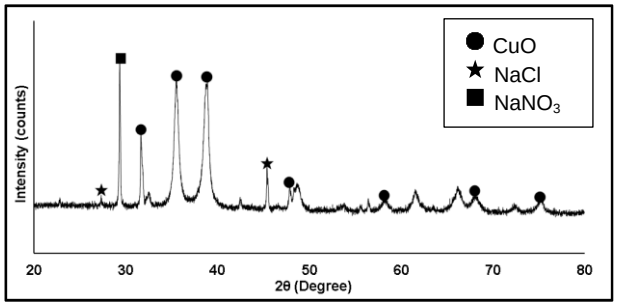

Figure 8. XRD pattern for CuO NPs

The prominent peaks for impurities present are labelled in Figure 8. The impurities that are present include nitratine ($NaNO_3$) and halide (NaCl), which were the salts formed after the precipitation of CuO NPs. Three times of washing process most likely did not remove all the salts present as past studies showed the decreased intensity of NO_3^{2-} molecules after 4 to 5 times of washing [17]. Besides that, among the precautionary step that can be taken in the future to ensure the salts and impurities was

removed is the usage of centrifugation to ensure that all the precipitates will be in contact with the ethanol-water mixture to remove the impurities. In addition, decomposition of $NaNO_3$ with the release of O_2 and NO can happen till the temperature of 680 °C. Thus, $NaNO_3$ might still be present after calcination at 450 °C [18]. The average crystalline size calculated through the Debye-Scherrer equation was 40.6 nm. The average crystalline size was calculated with the full width at half maximum (FWHM) where the smaller the width the greater the crystalline size.

3.6. Photocatalytic activity of CuO NPs

In this study, the photoefficiency of the synthesized CuO NPs as photocatalysts was tested out in the photodegradation of phenol as the model organic pollutant. The photocatalytic activity of the synthesized CuO NPs was tested out in the photodegradation of phenol under UV and visible light irradiations. The concentration of the phenol solution before and after irradiation was monitored with a UV-Vis spectrophotometer. First, 50 mL of the prepared 100 ppm phenol solution and 0.05 g of CuO NPs were stirred for 60 mins in dark conditions for adsorption. Then, around 8 mL of the solution was withdrawn with a syringe and filtered with a 0.45 µm syringe filter for analysis with the UV-Vis spectrophotometer. The sample was withdrawn and analyzed again after 5 h of irradiation with UV light under constant stirring. After that, the process was repeated by replacing the UV light source with the visible light source.

The UV-Vis spectra of the phenol solution with different concentrations and phenol calibration curve plots are shown in Figure 9 and Figure 10, respectively. The absorbance peak for phenol was located at 271 nm, which is in agreement with past studies [22]. The calibration plot was used to determine the concentration of the phenol solution versus time. The concentration of the phenol solution was identified through the calibration plot with the equation of $y = 0.001 x - 0.0138$ with an R^2 value of 0.995.

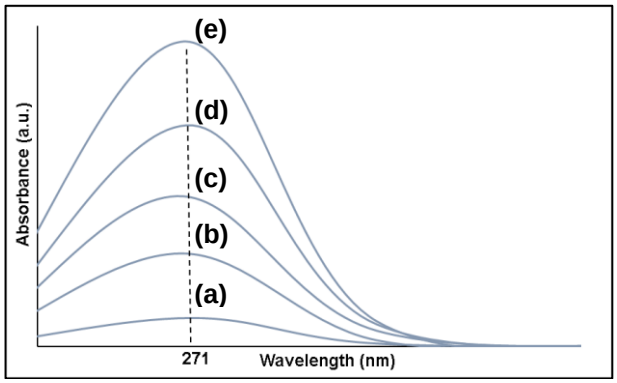

Figure 9. UV- Vis spectra of phenol at different concentrations; (a) 20 ppm, (b) 40 ppm, (c) 60 ppm, (d) 80 ppm and (e) 100 ppm

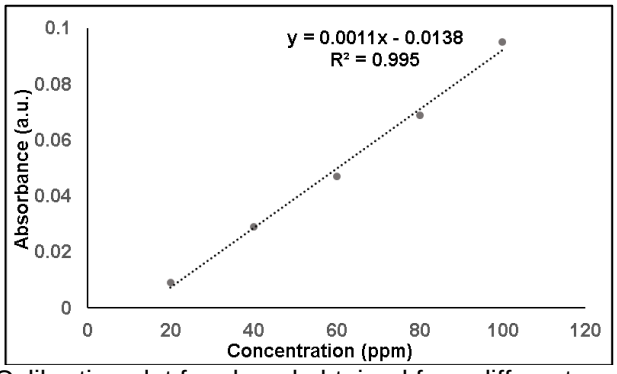

Figure 10. Calibration plot for phenol obtained from different concentrations

Figure 11 shows the degradation percentage of phenol under irradiation of UV and visible lights after 5 hours. The calculated degradation rate after 5 hours of irradiation under UV light was 45.3%

while for visible light the value was 58.5%. The degradation rate under visible light was higher than that of when UV light was used due to the value of the bandgap energy of the CuO NPs, which was in the visible light range . However, the degradation rate obtained was lower as compared to a past study in which the highest degradation rate of phenol under 60 mins of visible light irradiation was 98% [22].

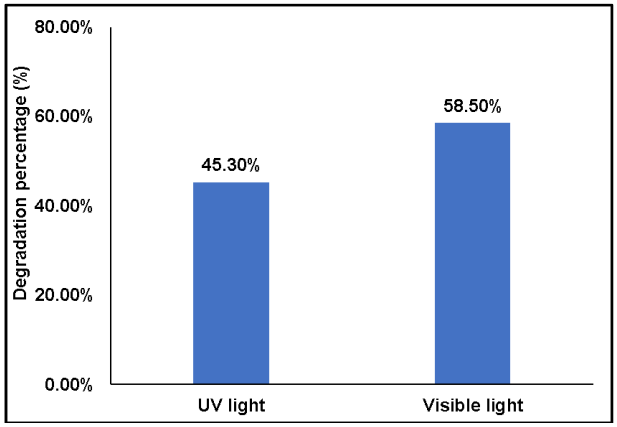

Figure 11. Degradation percentage of phenol after 5 hours of irradiation

One of the possible reasons that may affect the degradation rate was the crystalline size, where in the previous study, the size obtained was 24 nm, which was much smaller than the value obtained in this study. The higher value (40.6 nm) might be attributed to the clustering of nanoparticles after calcination. Different calcination temperatures and the presence of salts present in the CuO NPs might have caused the agglomeration of the crystal formed, which then increased the crystalline size [19].

Conclusion

In this study, CuO NPs had been successfully synthesized from waste SIM cards through a simple wet chemical method. The synthesized CuO NPs were characterized with FTIR for the identification of the functional groups, XRD for the crystallinity and NIR UV-Vis for the optical property. The XRD analysis showed that the CuO NPs synthesized in this study were in crystalline form with an average crystalline size of 40.6 nm. The FTIR spectrum showed the formation of CuO with peaks in the range of 400 to 600 cm^{-1} which corresponds to the Cu-O bond. The band gap energy of the CuO NPs was determined to be 2.1 eV, which is within the range of an efficient photocatalyst. The degradation rate of phenol under visible light irradiation (58.5%) was higher than that under UV light irradiation (45.3%). In short, it was proven that Cu metals from SIM cards can be extracted for the synthesis of CuO NPs and used as a photocatalyst in the degradation of phenol. This can effectively reduce the leaching of heavy metals from e-waste to the surrounding, while at the same time used to degrade organic pollutants such as phenol.

Acknowledgement

The authors would like to acknowledge funding from the Ministry of Education (MOE), Malaysia, through Fundamental Research Grant Scheme (FRGS/1/2021/STG04/UTM/02/2) and Kurita Asia Research Grant (22PMY153) provided by Kurita Water and Environment Foundation.

References

[1] Balde, C. P., Forti, V., Gray, V., Kuehr, R., Stegmann, & P. (2017). *Quantités, fl ux et ressources Suivi des déchets d'équipements électriques et électroniques à l'échelle mondiale 2017*.

[2] Ikhlayel, M. (2018). An integrated approach to establish e-waste management systems for developing countries. *Journal of Cleaner Production*, 170, 119–130.

[3] Krishnamoorthy, Y., Ma, V., Sakthivel, M., & Sarveswaran, G. (2018). Emerging public health threat of e-waste management: Global and Indian perspective. *Reviews on Environmental Health*, *33*(4), 321–329.

[4] Kiddee, P., Naidu, R., & Wong, M. H. (2013). Electronic waste management approaches: An overview. *Waste Management*, *33*(5), 1237–1250.
[5] Rene, E. R., Sethurajan, M., Kumar Ponnusamy, V., Kumar, G., Bao Dung, T. N., Brindhadevi, K., & Pugazhendhi, A. (2021). Electronic waste generation, recycling and resource recovery: Technological perspectives and trends. *Journal of Hazardous Materials*, *416*(February), 125-664.
[6] Beula, D., & Sureshkumar, M. (2021). A review on the toxic E-waste killing health and environment-Today's global scenario. *Materials Today: Proceedings*, 47, 2168–2174.
[7] Hubau, A., Minier, M., Chagnes, A., Joulian, C., Silvente, C., & Guezennec, A. G. (2020). Recovery of metals in a double-stage continuous bioreactor for acidic bioleaching of printed circuit boards (PCBs). *Separation and Purification Technology*, 238, 116481.
[8] Rajkumar, S., Elanthamilan, E., Balaji, T. E., Sathiyan, A., Jafneel, N. E., & Merlin, J. P. (2020). Recovery of copper oxide nanoparticles from waste SIM cards for supercapacitor electrode material. *Journal of Alloys and Compounds*, 849, 156582.
[9] Panda, R., Dinkar, O. S., Jha, M. K., & Pathak, D. D. (2020). Hydrometallurgical processing of waste multilayer ceramic capacitors (MLCCs) to recover silver and palladium. *Hydrometallurgy*, 197, 105476.
[10] Tran, T. H., & Nguyen, V. T. (2014). Copper Oxide Nanomaterials Prepared by Solution Methods, Some Properties, and Potential Applications: A Brief Review. *International Scholarly Research Notices*, *2014*, 1–14.
[11] Cuong, H. N., Pansambal, S., Ghotekar, S., Oza, R., Thanh Hai, N. T., Viet, N. M., & Nguyen, V. H. (2022). New frontiers in the plant extract mediated biosynthesis of copper oxide (CuO) nanoparticles and their potential applications: A review. *Environmental Research*, 203, 111858.
[12] Sahni, A., Kumar, A., & Kumar, S. (2016). Chemo-biohydrometallurgy—A hybrid technology to recover metals from obsolete mobile SIM cards. *Environmental Nanotechnology, Monitoring and Management*, 6, 130–133.
[13] Zayyoun, N., Bahmad, L., Laânab, L., & Jaber, B. (2016). The effect of pH on the synthesis of stable Cu2O/CuO nanoparticles by sol–gel method in a glycolic medium. *Applied Physics A*, *122*(5).
[14] Wahab, R., Siddiqui, M., Saquib, Q., Dwivedi, S., Ahmad, J., & Musarrat, J. et al. (2022). ZnO nanoparticles induced oxidative stress and apoptosis in HepG2 and MCF-7 cancer cells and their antibacterial activity.
[15] Chandrappa, K., & Venkatesha, T. (2013). Generation of nanostructured CuO by electrochemical method and its Zn-Ni-CuO composite thin films for corrosion protection. *Materials And Corrosion*, *64*(9), 831-839.
[16] Muhamad, R. Irmawati, A.H. Abdullah, Y.H Taufiq, Yap, S.B., Hamid (2007). Effect of Number of Washing on the Characteristics of Copper Oxide Nanopowders. *The Malaysian Journal of Analytical Sciences,* 11(1), 294-301.
[17] Hoshino, Y., Utsunomiya, T., & Abe, O. (1981). The Thermal Decomposition of Sodium Nitrate and the Effects of Several Oxides on the Decomposition. *Bulletin Of The Chemical Society Of Japan*, *54*(5), 1385-1391.
[18] Phiwdang, K., Suphankij, S., Mekprasart, W., & Pecharapa, W. (2013). Synthesis of CuO Nanoparticles by Precipitation Method Using Different Precursors. *Energy Procedia, 34, 740-745.*
[19] Dincer, I., & Rosen, M. A. (2021). *Thermal energy storage: systems and applications.* John Wiley & Sons.
[20] Wang, X., Yang, J., Shi, L., & Gao, M. (2016). Surfactant-free Synthesis of CuO with Controllable Morphologies and Enhanced Photocatalytic Property. *Nanoscale Research Letters*, 11(1).
[21] Dang, T., Le, S., Channei, D., Khanitchaidecha, W., & Nakaruk, A. (2016). Photodegradation mechanisms of phenol in the photocatalytic process. *Research On Chemical Intermediates*, *42*(6), 5961-5974.
[22] Nayak, R., Ali, F. A., Mishra, D. K., Ray, D., Aswal, V. K., Sahoo, S. K., & Nanda, B. (2020). Fabrication of CuO nanoparticle: An efficient catalyst utilized for sensing and degradation of phenol. *Journal of Materials Research and Technology*, 9(5), 11045–11059.